# GIS-Based DRASTIC and Composite DRASTIC Indices for Assessing Groundwater Vulnerability in the Baghin Aquifer, Kerman, Iran

Mohammad Malakootian[1], Majid Nozari[2,*]

**Manuscript Authors details:**

1. Mohammad Malakootian, Department of Environmental Health, School of Public Health, Kerman University of Medical Sciences, Iran. E-mail: m.malakootian@yahoo.com. https://orcid.org/0000-0002-4051-6242.

2. Majid Nozari, Department of Environmental Health, School of Public Health, Kerman University of Medical Sciences, Iran. Tel: 98-9383921819, E-mail: nozari.m@kmu.ac.ir. https://orcid.org/0000-0003-2319-1930.

## ABSTRACT

The present study estimated the Kerman–Baghin aquifer vulnerability using DRASTIC and composite DRASTIC (CDRASTIC) indices with the aid of geographic information system (GIS) techniques. Factors affecting the transfer of contamination, including water table depth, soil media, aquifer media, the impact of the vadose zone, topography, hydraulic conductivity, and land use were used to calculate the DRASTIC and CDRASTIC indices. A sensitivity test was also performed to determine the sensitivity of the parameters. Results showed that the topographic layer displays a gentle slope in the aquifer. Most of the aquifer was covered with irrigated field crops and grassland with a moderate vegetation cover. In addition, the aquifer vulnerability maps indicated very similar results, identifying the northwest parts of the aquifer as areas with high to very high vulnerability. The map removal sensibility analysis (MRSA) revealed the impact of the vadose zone (in the DRASTIC index) and hydraulic conductivity (in

the CDRASTIC index) as the most important parameters in vulnerability evaluation. In both indices, the single-parameter sensibility analysis (SPSA) demonstrated net recharge as the most effective factor in vulnerability estimation. According to the results, parts of the studied aquifer have a high vulnerability and require protective measures.

**Keywords:** Vulnerability; Sensitivity Analysis; DRASTIC; Composite DRASTIC; Kerman–Baghin Aquifer

## 1. Introduction

Groundwater is a significant and principal freshwater resource in most parts of the world, especially in arid and semi-arid areas. Water quality has been emphasized in groundwater management (Neshat et al., 2014; Manap et al., 2013; Manap et al., 2014a; Ayazi et al., 2010). The potential groundwater contamination by human activities at or near the surface of groundwater has been considered the major basis for managing this resource by implementing preventative policies (Tilahun and Merkel, 2010).

Groundwater vulnerability is a measure of how easy it is for pollution or contamination at the land surface to reach a production aquifer. In other words, it is a measure of the "degree of insulation" that natural and artificial factors provide to keep pollution away from the groundwater (Sarah and Patricia, 1993; Neshat et al., 2014). Vulnerability maps are commonly plotted at the sub-region and regional scales. Normally, they are not applied to site-specific evaluations, including zones smaller than a few tens of square kilometers (Baalousha, 2006; Tilahun and Merkel, 2010). Various techniques have been developed to assess groundwater susceptibility with great precision (Javadi et al., 2010; Javadi et al., 2011). Most of these techniques are based on analytic tools to associate groundwater contamination to land operations.

45 There are three types of evaluation methods: process-based simulations, statistic procedures, and
46 overlay and index approaches (Neshat et al., 2014; Dixon, 2004).

47 Process-based approaches involve numerical modeling and are useful at the local but not at
48 the regional level. Statistical approaches involve correlating actual water quality data to spatial
49 variables and require a large amount of site-specific data (National Research Council, 1993).
50 Overlay and index procedures emphasize the incorporation of various zonal maps by allocating a
51 numeral index. Both procedures are simple to implement in the geographic information system
52 (GIS), especially on a zonal measure. Hence, these methods are the most popular procedures
53 applied forvulnerability estimation (Neshat et al., 2014). The overlay and index methods have
54 some significant advantages; first, they have become popular because the methodology is fairly
55 straightforward and can be easily implemented with any GIS application software. The concept
56 of overlaying data layers is easily comprehensible, even by less experienced users. In addition,
57 the data requirement can be considered as moderate, since nowadays most data come in a digital
58 format. Hydrogeological information is either available or could be estimated using relevant
59 data. Consequently, these methods yield relatively accurate results for extensive areas with a
60 complex geological structure. Last, the product of this approach could be easily interpreted by
61 water-resource managers and incorporated into decision-making processes. Even a simple visual
62 inspection of the vulnerability map can reveal important contamination hotspots. Probably the
63 most important and obvious disadvantage of these methods raised by scientists and experts is the
64 inherent subjectivity in the determination of the rating scales and the weighting coefficients
65 (National Research Council, 1993).

66 The most extensively used methods for groundwater vulnerability evaluation are GODS
67 (Ghazavi and Ebrahimi, 2015), IRISH (Daly and Drew, 1999), aquifer vulnerability index (AVI)

(Raju et al., 2014), and DRASTIC (Neshat et al., 2014; Baghapour et al., 2014; Baghapour et al., 2016).

The DRASTIC index, proposed by Aller et al. (1985), is regarded as one of the best indices for groundwater vulnerability estimation. This method ignores the influence of zonal properties. Thus, identical weights and rating values are utilized. In addition, this technique fails to apply a standard validation test for the aquifer. Therefore, several investigators developed this index using various techniques (Neshat et al., 2014). A higher DRASTIC index represents a greater contamination potential, and vice versa. After calculating the DRASTIC index, it should be possible to identify the zones that are more prone to pollution. This index only provides a relative estimation and is not created to make a complete assessment (Baalousha, 2006).

Many studies have been conducted using the DRASTIC index to estimate groundwater vulnerability in different regions of the world (Jaseela et al., 2016; Zghibi et al., 2016; Kardan Moghaddam et al., 2017; Kumar et al., 2016; Neshat and Pradhan, 2017; Souleymane and Tang, 2017; Ghosh and Kanchan, 2016; Saida et al., 2017); however, there are still a number of studies that have employed the CDRASTIC index for groundwater vulnerability evaluation (Baghapour et al., 2016; Baghapour et al., 2014; Secunda et al., 1998; Jayasekera et al., 2011; Shirazi et al., 2012; Jayasekera et al., 2008). Boughriba et al. (2010) utilized the DRASTIC index in a GIS environment to estimate aquifer vulnerability. They provided the DRASTIC-modified map prepared from total DRASTIC indices and small monitoring network maps including high and medium classes. Then, they integrated the map with a land use map to prepare a contamination potential map. They reported the newly obtained groundwater vulnerability map, including three classes, namely very high, high, and medium. Babiker et al. (2005) used the DRASTIC index to determine the points prone to contamination from human activities in the aquifer. They reported

that the western and eastern parts of the aquifer fall in the high and medium classes, respectively, in terms of vulnerability. The final aquifer vulnerability map represented that a high risk of pollution is found in the eastern part of the aquifer due to agricultural activities. They also observed that net recharge inflicts the largest impact on aquifer vulnerability, followed by soil media, topography, the impact of the vadose zone, and hydraulic conductivity.

The average annual precipitation in Iran is 257 mm (less than one-third of the average annual precipitation at the global level). Water scarcity is a critical problem in Iran (Chitsazan and Akhtari, 2006; Modabberi et al., 2017), and groundwater reduction has exacerbated the problem. Groundwater is the only freshwater resource in Kerman Province, Iran, due to the lack of surface water. The Baghin aquifer is located in the central part of Kerman Province. Due to recent droughts, this aquifer has been under heavy pumping stress to irrigate crops, which caused a gradual drop inwater level. Consequently, this could increase the contamination potential by changing the physical and chemical properties of water in the aquifer. Therefore, the aim of this research was to provide a vulnerability map for the Kerman–Baghin aquifer and perform a sensitivity analysis to identify the most influential factors in vulnerability assessment.

## 2. Materials and Methods

### 2.1.Study Area

The Kerman province covers both arid and semi-arid lands. The present study included a 2023-km$^2$area (29◦ 47′ to 30◦ 31′ N latitude and 56◦ 18′ to 57◦ 37′ E longitude) located in the central part of Kerman Province (Figure 1). The study area is mostly covered with agricultural lands (Neshat et al., 2014). The mean annual rainfall is 108.3 mm (during 2017) in the study area; the highest and lowest topographic elevation is 1,980 and 1,633 m above the sea level, respectively;

and the mean, minimum, and maximum annual temperatures equal 17°C, -12°C, and 41°C, respectively (during 2017).

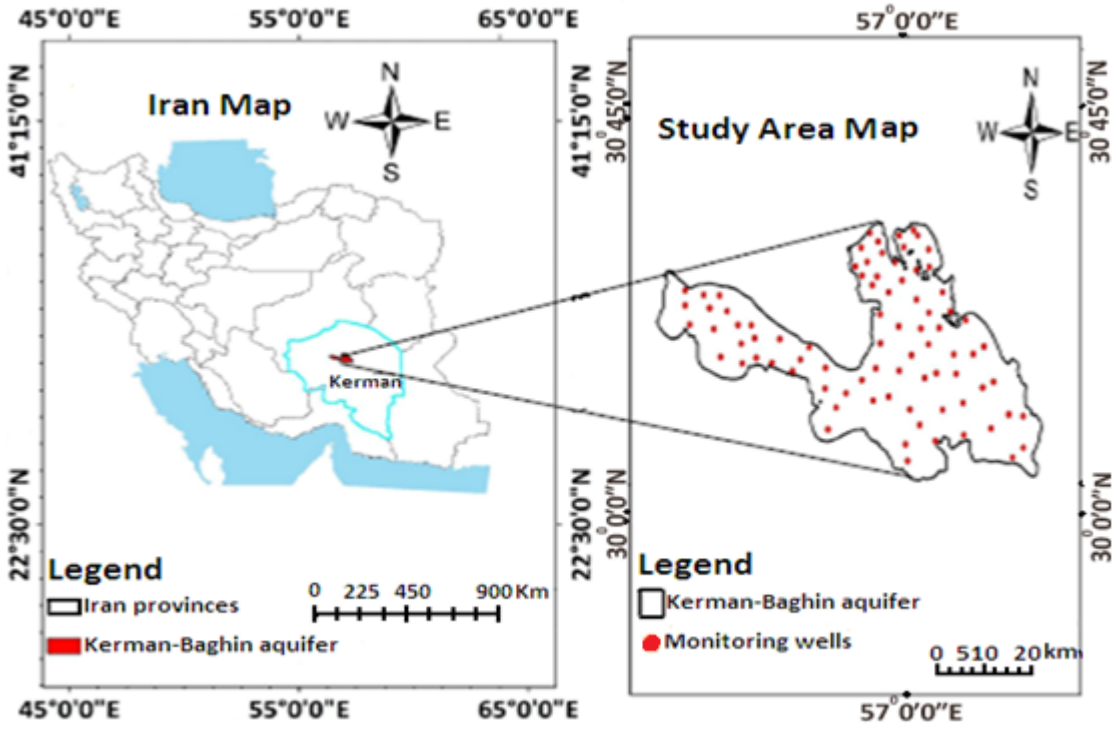


**Figure 1.** Location map of the Kerman–Baghin aquifer

## 2.2. Computation of DRASTIC and CDRASTIC Indices

DRASTIC is a procedure developed by the United States Environmental Protection Agency (U.S. EPA) to evaluate groundwater pollution (Aller et al., 1985). The DRASTIC index is obtained using the following equation (Kardan Moghaddam et al., 2017; Neshat and Pradhan, 2017):

$$\text{DRASTIC index} = D_r D_w + R_r R_w + A_r A_w + S_r S_w + T_r T_w + I_r I_w + C_r C_w, \quad (1)$$

where DRASTIC comprises the effective factors in the DRASTIC index; D, R, A, S, T, I, and C stand for water table depth, net recharge, aquifer media, soil media, topography, the impact of the vadose zone, and hydraulic conductivity, respectively; and "*r*" and "*w*" denote the rating and

weight of each factor, respectively. The ratings and weights of the factors are presented in Table 1. A high DRASTIC index corresponds to the high vulnerability of the aquifer to pollution. In the DRASTIC index, each parameter is rated on a scale from 1 to 10 that shows the relative contamination potential of that parameter for that area. In addition, in the DRASTIC index, one weight (1 to 5) is assigned to each parameter. Weight values indicate the relative significance of the parameters with respect to one another. Ranges of vulnerability corresponding to the DRASTIC index are presented in Table 2.

**Table 1** Ratings and weights related to DRASTIC index factors (Aller et al., 1985)

| DRASTIC parameters | Range | Rating (r) | Weight (w) |
|---|---|---|---|
| Water table depth (m) | 0.0-1.5 | 10 | |
| | 1.5-4.6 | 9 | |
| | 4.6-9.1 | 7 | |
| | 9.1-15.2 | 5 | 5 |
| | 15.2-22.9 | 3 | |
| | 22.9-30.5 | 2 | |
| | >30.5 | 1 | |
| Net recharge | 11-13 | 10 | |
| | 9-11 | 8 | |
| | 7-9 | 5 | 4 |
| | 5-7 | 3 | |
| | 3-5 | 1 | |
| Aquifer media | Rubble and sand | 9 | |
| | Gravel and sand | 7 | |
| | Gravel, sand, clay, and silt | 5 | 3 |
| | Sand and clay | 4 | |
| | Sand, clay, and silt | 3 | |
| Soil media | Rubble, sand, clay, and silt | 9 | |
| | Gravel and sand | 7 | |
| | Gravel, sand, clay, and silt | 6 | |
| | Sand | 5 | 2 |
| | Sand, clay, and silt | 3 | |
| | clay and silt | 2 | |
| Topography or slope (%) | 0-2 | 10 | |
| | 2-6 | 9 | |
| | 6-12 | 5 | 1 |
| | 12-18 | 3 | |
| | >18 | 1 | |

| | | | |
|---|---|---|---|
| The impact of the vadose zone | Rubble, sand, clay, and silt | 9 | |
| | Gravel and sand | 7 | |
| | Gravel, sand, clay, and silt | 5 | 5 |
| | Sand, clay, and silt | 3 | |
| Hydraulic conductivity (m/day) | 0-4.1 | 1 | |
| | 4.1-12.2 | 2 | 3 |
| | 12.2-28.5 | 4 | |
| | 28.5-40.7 | 6 | |
| | 40.7-81.5 | 8 | |

**Table 2** Range of vulnerability related to the DRASTIC index

| Vulnerability | Ranges |
|---|---|
| Very low | 23-46 |
| Low | 47-92 |
| Moderate | 93-136 |
| High | 137-184 |
| Very high | >185 |

In the CDRASTIC index , the DRASTIC index parameters modified by adding a new parameter called land use. Then, the role of land use in aquifer vulnerability potential is determined. The CDRASTIC index was obtained as follows:

$$\text{CDRASTIC index} = D_r D_w + R_r R_w + A_r A_w + S_r S_w + T_r T_w + I_r I_w + C_r C_w + L_r L_w, \quad (2)$$

where $L_w$ and $L_r$ are the relative weight and rating related to land use, respectively. Ratings and weightings applied to the pollution potential are presented in Table 3 and are related to land use based on the CDRASTIC index. The final outputs of the CDRASTIC index range from 28 to 280. Vulnerability ranges based on the CDRASTIC index are presented in Table 4.

**Table 3** Ratings and weighting applied to the pollution potential related to land use based on the CDRASTIC index (Aller et al., 1985)

| Land use | Rating | Weight |
|---|---|---|
| Irrigated field crops + Urban areas | 10 | |
| Irrigated field crops + Grassland with poor vegetation cover + Urban areas | 9 | |
| Irrigated field crops + Grassland with moderate vegetation cover + Urban areas | 8 | |
| Irrigated field crops | 8 | |
| Irrigated field crops + Fallow land + Grassland with poor vegetation cover | 7 | |
| Irrigated field crops + Grassland with poor vegetation cover | 7 | |
| Irrigated field crops + Grassland with moderate vegetation cover | 6 | |

| | | |
|---|---|---|
| Irrigated field crops + Rocky + Urban areas | 5 | 5 |
| Irrigated field crops + Grassland with poor vegetation cover + Woodland | 5 | |
| Irrigated field crops + Woodland | 5 | |
| Irrigated field crops + Rocky | 4 | |
| Fallow land | 3 | |
| Fallow land + Grassland with poor vegetation cover | 3 | |
| Fallow land + Grassland with moderate vegetation cover | 3 | |
| Grassland with poor vegetation cover | 2 | |
| Grassland with moderate vegetation cover | 2 | |
| Grassland with moderate vegetation cover + Woodland | 1 | |
| Sand dune +Grassland with moderate vegetation cover | 1 | |
| Sand dune | 1 | |

**Table 4** Vulnerability ranges related to the CDRASTIC index

| Vulnerability | Ranges |
|---|---|
| Very low | <100 |
| Low | 100-145 |
| Moderate | 145-190 |
| High | 190-235 |
| Very high | ≥235 |

### 2.3. Factors Affecting the Transfer of Contamination

Water table depth is the distance of the water table from the ground surface in a well (Baghapour et al., 2016). Eighty-three wells were utilized in the Kerman–Baghin aquifer to obtain this factor. The interpolation procedure was adopted to provide a raster map of the water table depth, which was categorized based on Table 2.

Net recharge is the amount of runoff that has penetrated into the ground and has reached the groundwater surface (Singh et al., 2015; Ghosh and Kanchan, 2016). This research used the Piscopo method (Chitsazan and Akhtari, 2009) to provide a net recharge layer for the Kerman–Baghin aquifer according to the following equation and Table 5:

$$\text{Net recharge} = \text{slope}\ (\%) + \text{rainfall} + \text{soil permeability}. \quad (3)$$

In the above equation, the percentage of the slope was calculated from a topographical map, using a digital elevation model. In addition, a soil permeability map was created using the

158 Kerman–Baghin aquifer soil map (scale of 1:250000) and the drilling logs of 83 wells. Finally, a
159 map of the rainfall rate in the area was plotted based on annual average precipitation. The ratings
160 and weights of net recharge are presented in Table 5.

161 **Table 5** Weight, rating, and range of net recharge (Aller et al., 1985)

| Slope (%) | | Rainfall | | Soil permeability | | Net Recharge | | |
|---|---|---|---|---|---|---|---|---|
| Range (%) | **Factor** | Range (mm/year) | **Factor** | Range | **Factor** | Range (cm/year) | **Rating** | **Weight** |
| <2 | 4 | >850 | 4 | High | 5 | 11-13 | 10 | |
| 2-10 | 3 | 700-850 | 3 | Moderate to high | 4 | 9-11 | 8 | |
| 10-33 | 2 | 500-700 | 2 | Moderate | 3 | 7-9 | 5 | 4 |
| >33 | 1 | <500 | 1 | Low | 2 | 5-7 | 3 | |
| | | | | Very low | 1 | 3-5 | 1 | |

162 Aquifer media controls the movement of groundwater streams in the aquifer (Aller et al.,
163 1985; Singh et al., 2015). To obtain this layer, the drilling log data of 83 wells were used. Data
164 were collected from the Kerman Regional Water Office (KRWO). The range of the aquifer
165 media layer is shown in Table 2.

166 Soil media has a considerable impact on the amount of water surface that can penetrate the
167 aquifer. Therefore, where the soil layer is thick, the debilitation processes such as absorption,
168 filtration, degradation, and evaporation may be considerable (Singh et al., 2015). A soil media
169 raster map was provided using the Kerman–Baghin aquifer soil map and the wells' drilling logs.
170 The range of the soil media layer is presented in Table 2.

171 Topography controls the residence time of water inside the soil and the degree of penetration
172 (Singh et al., 2015). To obtain this layer, the percentage of the slope was obtained from the
173 topographical map, using a digital elevation model. Data were collected from the KRWO. The
174 range of the topographic layer is presented in Table 2.

175 A vadose zone is an unsaturated area located between the topographic surface and the
176 groundwater level (Singh et al., 2015). It plays a significant role in decreasing groundwater

177 contamination by pollutant debilitation processes such as purification, chemical reaction, and
178 dispersal (Shirazi et al., 2012). This study used the lithologic data of 83 observation and
179 exploration wells to design the impact of thevadose zone raster map of the aquifer. The data
180 were collected from the KRWO. The range of the impact of thevadose zone layer is depicted in
181 Table 2.

182 Hydraulic conductivity refers to the capability of the aquifer to transfer water. Areas with a
183 high hydraulic conductivity demonstrate a high potential for groundwater contamination (Singh
184 et al., 2015; Aller et al., 1985). To prepare this layer, data derived from pumping tests of wells
185 were used. The range of the hydraulic conductivity layer is given in Table 2.

186 Land use affects groundwater resources through changes in recharge and by changing demands
187 for water .Land use is obligatory since it is required by the CDRASTIC index. The Indian remote
188 sensing satellite information was utilized to create the land use raster map. The weight and rating
189 related to the land use layer are presented in Table 3.

190 **2.4. Sensitivity Analyses**

191 One of the main advantages of the DRASTIC index is the evaluation performance because a high
192 number of input data are used, and this helps restrict the effects of errors on final results.
193 Nevertheless, some authors, namely Babikeret al. (2005), Barber et al. (1993), and Merchant
194 (1994), reported that similar results could be obtained using fewer data and at lower costs. The
195 unavoidable subjectivity related to the selection of seven factors, ranks, and weights used to
196 calculate the vulnerability index has also been criticized. Therefore, in order to eliminate the
197 aforementioned criticisms, two sensitivity analyses were performed as follows (Napolitano and
198 Fabbri, 1996):

199 **A. Map Removal Sensibility Analysis (MRSA)**

MRSA value indicates the vulnerability map's sensibility to the removal of one or more maps from the suitability analysis. MRSA is calculated as follows (Babiker et al., 2005; Martínez-Bastida et al., 2010; Saidi et al., 2011; Modabberi et al., 2017):

$$S = \left[\left|\frac{\frac{V}{N} - \frac{V'}{n}}{V}\right|\right] \times 100, \quad (4)$$

where S stands for the sensibility value expressed in terms of the variation index, V is the intrinsic vulnerability index (real vulnerability index), V′ is the intrinsic vulnerability index after removing X, and N and n are the number of data pieces used to calculate V and V′, respectively (Babiker et al., 2005; Martínez-Bastida et al., 2010; Saidi et al., 2011; Modabberi et al., 2017).

**B. Single-Parameter Sensibility Analysis (SPSA)**

SPSA was first introduced by Napolitano and Fabbri (1996). This test shows the effect of each DRASTIC factor on the final vulnerability index. Using this test derived from Equation 5, the real and effective weight of each factor, compared to the theoretical weight assigned by the analytical model, was calculated by Babiker et al. (2005), Martínez-Bastida et al.(2010), Saidi et al. (2011), and Modabberi et al.(2017);

$$W = \left[\frac{P_r P_w}{V}\right] \times 100, \quad (5)$$

where W represents the effective weight of each factor, $P_r$ and $P_w$ are the rank and weight assigned to P, respectively, and V denotes the intrinsic vulnerability index (Martínez-Bastida et al., 2010; Babiker et al., 2005; Saidi et al., 2011; Modabberi et al., 2017).

## 3. Results and Discussion

### 3.1. DRASTIC and CDRASTIC Parameters

Based on the data shown in Table 2, the assigned rating of water table depth varies from 1 to 10. In addition, based on the results presented in Table 6, water table depth in the aquifer varies from

4.6 to >30.5 m (rating 1 to 7). About 27.55% of the aquifer has a depth >30.5 m, and 66.16% of the aquifer has a depth ranging from 9.1 m to30.5 m. Less than 7% of the aquifer has a depth between 4.6 m and 9.1 m. The Kerman–Baghin aquifer rated map of water table depth is depicted in Figure 2(A). According to Figure 2(A) and Table 6, the minimum impact of water table depth on aquifer vulnerability occurs in the central parts (6.39%), whereas the maximum impact occurs in the northern, southern, northwestern, and southeastern parts (27.55%).

According to the results presented in Table 6, 75.81% of the aquifer has a net recharge value of7 to 9 cm/year. A net recharge value between 9 and 11 cm/year was found for 11.74% of the aquifer. The Kerman–Baghin aquifer rated map of net recharge is illustrated in Figure 2(B). According to Piscopo's method, the Kerman–Baghin aquifer was divided into three classes with regard to net recharge. The highest net recharge value was observed in the northern, northeastern, southern, and southwestern parts of the northwest, parts of the center, and parts of the southeast (75.81%), whereas the least net recharge value appeared in parts of the northwest and center (11.74%), as shown in Figure 2(B) and Table 6.

As observed in Table 6, the majority of the Kerman–Baghin aquifer media is composed of sand, clay, and silt (75.21%). The Kerman–Baghin aquifer rated map of the aquifer media is presented in Figure 3(A). Parts of the aquifer in the north, northwest, northeast, center, and southeast are composed of sand, clay, and silt. Parts of the aquifer in the northwest are composed of rubble and sand (5.58%). Parts of the aquifer in the south and northwest are composed of gravel and sand (8.95%), and gravel, sand, clay, and silt (10.26%).

The Kerman–Baghin aquifer rated map of soil media is presented in Figure 3(B). The soil map depicts six soil classes. The highest rank (rank = 9) was assigned to rubble, sand, clay, and silt (a combination of rubble, sand, clay and silt soils). In addition, the lowest rank (rank = 2) was

assigned to clay and silt (a combination of clay and silt soils). Most of the aquifer soil media is covered with silt, sand, and clay (about 80%).

The Kerman–Baghin aquifer rated map of topography is shown in Figure 4(A). The topographical layer demonstrates a gentle slope (0 to 6%) over most of the aquifer, hence gaining the ranks of 9 and 10. A slope range of 0 to 2% includes 34.72% of the study area, and its rating (slope range = 0–2%) is 10. In addition, 65.28% of the aquifer has a slope range of 2 to 6% (parts of the northwest) as shown in Figure 4(A) and Table 6. As the gradient increases, the runoff increases as well (Israil et al., 2006), leading to less penetration (Jaiswal et al., 2003). According to Madrucci et al. (2008), the gradients higher than 35° are considered restrictions on groundwater desirability because of the lack of springs.

The Kerman–Baghin aquifer rated map of the impact of the vadose zone is indicated in Figure 4(B). According to the results, the soil with a rank of 5 (gravel, sand, clay, and silt) is more effective on aquifer vulnerability (35.47%). Other types of soils such as sand, clay, and silt (parts of the north, northeast, south, and southeast), gravel and sand (parts of the center and northwest), and rubble, sand, clay, and silt (parts of the northwest) cover 34.24%, 20.39%, and 9.9% of the aquifer, respectively, as shown in Figure 4(B) and Table 6. Sandy soil is effective on groundwater occurrence because of the high rate of penetration (Srivastava and Bhattacharya, 2006). However, clay soil is arranged poorly because of low infiltration (Manap et al., 2014b).

The Kerman–Baghin aquifer rated map of hydraulic conductivity is illustrated in Figure 5(A). Hydraulic conductivity shows a high degree of variability. The findings showed that the hydraulic conductivity of the Kerman–Baghin aquifer varies from 0 to 81.5 m/day. The potential for groundwater contamination was greater in zones with high hydraulic conductivity (38.27%). As shown in Figure 5(A) and Table 6, 29.51%, 23.93%, 5.98%, and 2.31% of the study areas

have hydraulic conductivity in the ranges of 0 to 4.1 m/day, 12.2 to 28.5 m/day, 28.5 to 40.7 m/day, and 40.7 to 81.5 m/day, respectively.

The Kerman–Baghin aquifer rated map of land use is presented in Figure 5(B). The results indicated that the majority of the Kerman–Baghin aquifer is covered with irrigated field crops and grassland with a moderate vegetation cover (20.45%). Less than 4% of the study area is composed of irrigated field crops and urban areas (3.61%), and 58.47% of the study area consists of irrigated field crops with urban areas, grassland with poor and moderate vegetation cover, fallow land, woodland, and rocky ground. In addition, 10.17% of the study area is fallow land with poor grassland and moderate vegetation, and 13.72% of the study area is sand dunes with poor grassland and moderate vegetation cover and woodland, as displayed in Figure 5(B) and Tables 3 and 6.

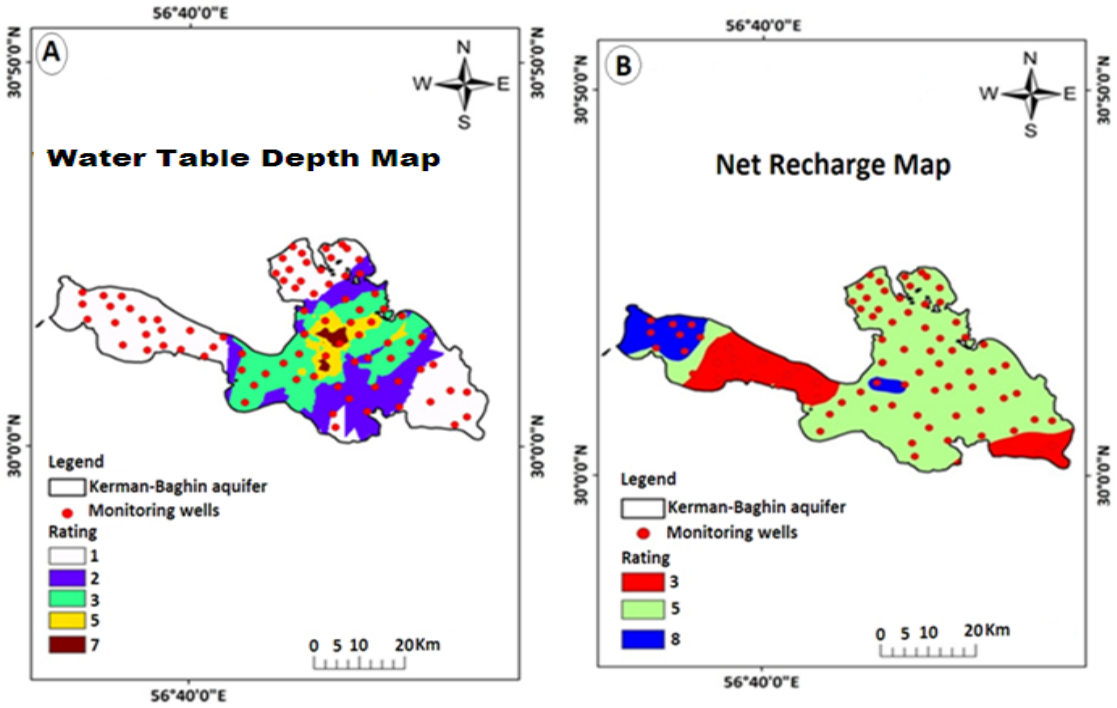


**Figure 2.** The Kerman–Baghin aquifer rated maps of A) water table depth and B) net recharge

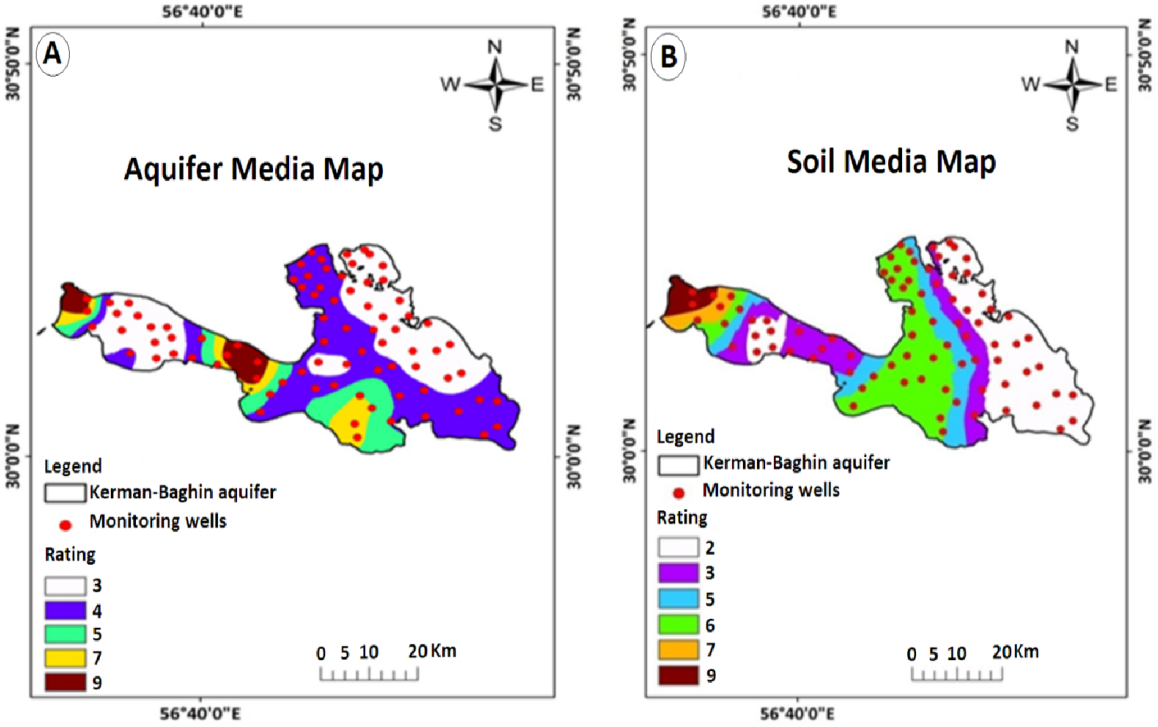


**Figure 3.** The Kerman–Baghin aquifer rated maps of A) aquifer media and B) soil media

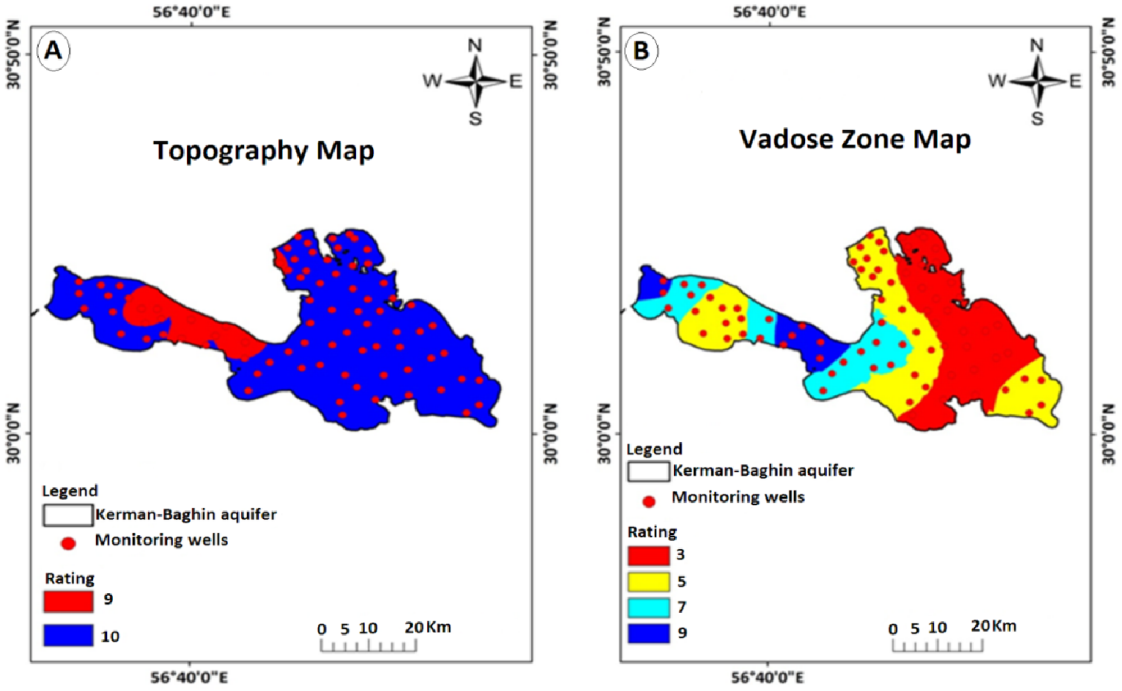


**Figure. 4.** The Kerman–Baghin aquifer rated maps of A) topography and B) vadose zone

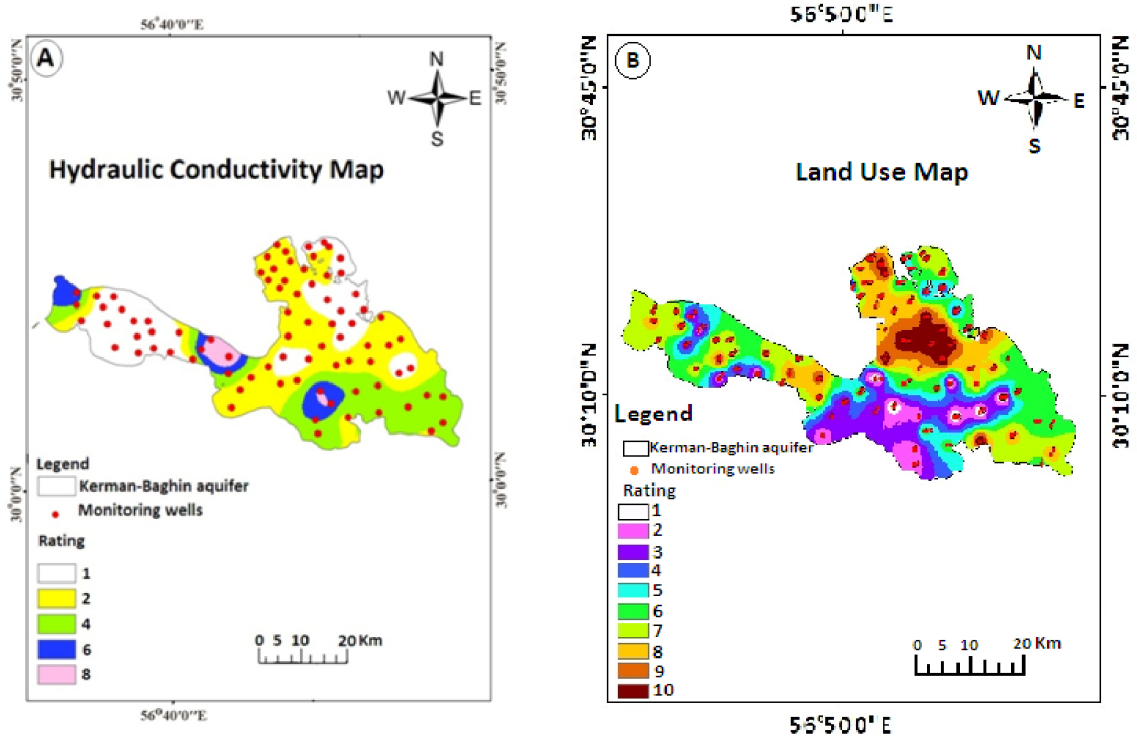


285

286 **Figure. 5.** The Kerman–Baghin aquifer rated maps of A) hydraulic conductivity and B) land use

287 **Table 6** Area of rating ($km^2$ and %) of DRASTIC and CDRASTIC parameters

| DRASTIC and CDRASTIC indexes parameters | Rating | Area ($km^2$) | Area (%) | The aquifer geographic directions covered by the respective rating in the parameters rated maps |
|---|---|---|---|---|
| **Water table depth** | 1 | 557.73 | 27.55 | Parts of the north, south, northwest, and southeast |
| | 2 | 472.18 | 23.34 | Parts of the north, south, and center |
| | 3 | 469.78 | 23.29 | Parts of the center |
| | 5 | 395.00 | 19.53 | Parts of the center |
| | 7 | 129.14 | 6.39 | Parts of the center |
| **Net recharge** | 3 | 252.04 | 12.45 | Parts of southeast, and northwest |
| | 5 | 1534.15 | 75.81 | North, northeast, south, southwest, and parts of the northwest, center, southeast |
| | 8 | 237.6 | 11.74 | Parts of the northwest and center |
| **Aquifer media** | 3 | 743.18 | 36.72 | Parts of the north, northwest, northeast, and center |
| | 4 | 779.01 | 38.49 | Parts of the north, northwest, southeast, and center |
| | 5 | 207.81 | 10.26 | Parts of the south, and northwest |
| | 7 | 181.02 | 8.95 | Parts of the south, and northwest |
| | 9 | 112.76 | 5.58 | Parts of the northwest |
| **Soil media** | 2 | 658.5 | 32.53 | Parts of the north, northwest, northeast, and southeast |
| | 3 | 399.72 | 19.75 | Parts of the north, northwest, south, and center |
| | 5 | 297.44 | 14.69 | Parts of the north, northwest, south, and center |
| | 6 | 538.77 | 26.62 | Parts of the northwest, center, and southwest |

| | | | | |
|---|---|---|---|---|
| | 7 | 67.56 | 3.33 | Parts of the northwest |
| | 9 | 61.79 | 3.08 | Parts of the northwest |
| **Topography** | 9 | 702.74 | 34.72 | North, northwest, northeast, south, southeast, southwest, and center |
| | 10 | 1321.07 | 65.28 | parts of the northwest |
| **The impact of the** | 3 | 692.87 | 34.24 | Parts of the north, northeast, south, and southeast |
| **vadose zone** | 5 | 717.91 | 35.47 | Parts of the north, northwest, south, southeast, and center |
| | 7 | 412.49 | 20.39 | Parts of the center, and northwest |
| | 9 | 200.53 | 9.9 | Parts of the northwest |
| **Hydraulic** | 1 | 597.11 | 29.51 | Parts of the northeast, northwest, southeast, and center |
| **conductivity** | 2 | 774.52 | 38.27 | parts of the northwest, south, southeast, and center |
| | 4 | 484.17 | 23.93 | Parts of the northwest, south, and southeast |
| | 6 | 120.99 | 5.98 | Parts of the south, and northwest |
| | 8 | 46.7 | 2.31 | Parts of the south, and northwest |
| **Land use** | 1 | 112.48 | 5.56 | Parts of the south |
| | 2 | 165.02 | 8.16 | Parts of the south |
| | 3 | 205.65 | 10.17 | Parts of the south, and center |
| | 4 | 357.06 | 17.64 | Parts of the south, southwest, northwest, and center |
| | 5 | 234.86 | 11.61 | Parts of the southeast, northwest, and center |
| | 6 | 413.86 | 20.45 | Parts of the southeast, northwest, northeast, and center |
| | 7 | 182.63 | 9.02 | Parts of the north, northwest, and northeast |
| | 8 | 169.4 | 8.37 | Parts of the north, northwest, and northeast |
| | 9 | 109.42 | 5.41 | Parts of the north, northwest, and northeast |
| | 10 | 73.09 | 3.61 | Parts of the north |

### 3.2. DRASTIC and CDRASTIC Vulnerability Indices

The Kerman–Baghin aquifer vulnerability map obtained using DRASTIC and CDRASTIC indices are given in Figure 6. In the studied aquifer, vulnerability falls under very high, high, moderate, low, and very low vulnerable areas. It is found that in both indices, the northern, northeastern, northwestern, southern, southwestern, southeastern, and central parts are classified as having low and very low vulnerability. This could be attributed to the low water depth, hydraulic conductivity, and net recharge characterizing these aquifer areas; another reason might be that the aquifer media is mostly clay, sand, and silt soils. The vulnerability area, identified by the investigated indices, is illustrated in Table 7. Zones with a low and very low vulnerability cover 25.21% and 38.31%of the Kerman–Baghin aquifer, respectively, using DRASTIC index. Very low and low-vulnerability zones cover 24.95% and 40.41%, respectively, using the CDRASTIC index. This is primarily due to water table depth and the relatively low permeability

of the vadose zone in those aquifers (Colins et al., 2016). About 26% of the studied aquifer had moderate groundwater pollution potential, using DRASTIC and CDRASTIC indices. This does not mean that these areas are without pollution; rather, they are relatively prone to pollution when compared to other areas (Colins et al., 2016). From the DRASTIC index values, it was found that 10.4% of the studied aquifer had high (8.46%) and very high (1.94%) vulnerability. The results revealed that 8.75% of the aquifer fell in the range of 190 to 235 and greater than 235 in the CDRASTIC index (Table 7). According to these two indices, the vulnerability maps indicated very similar findings, suggesting that the northwestern part of the aquifer has zones with high and very high vulnerability. The high vulnerability can be attributed to great water depth, hydraulic conductivity, and net recharge in these aquifer areas. In addition, this can due to the great slope in this area.

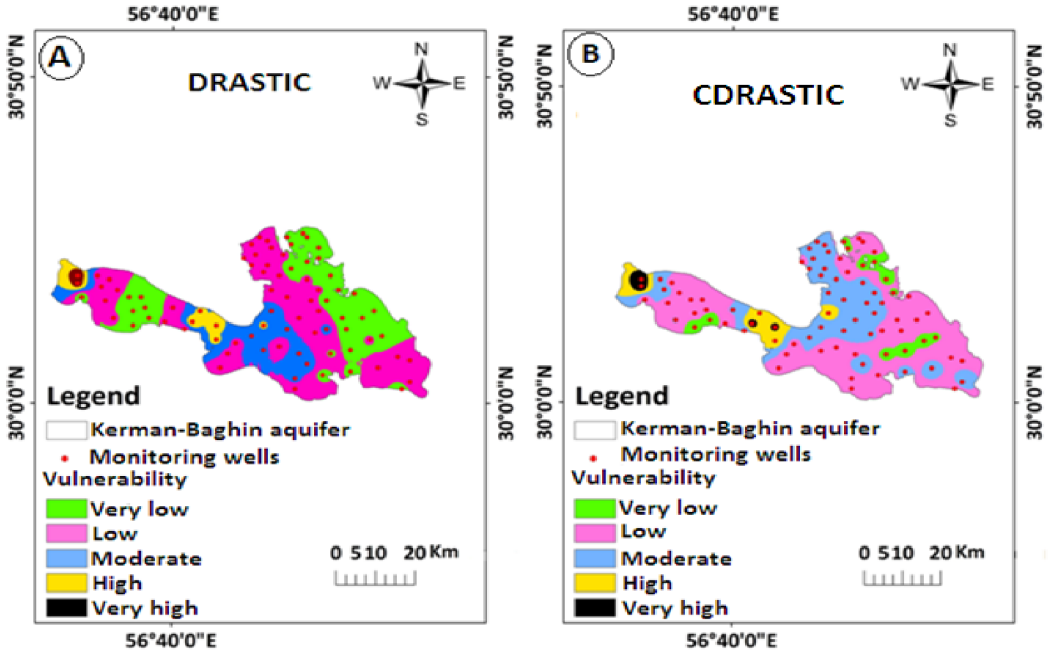


**Figure 6.** Vulnerability maps of the Kerman–Baghin aquifer by DRASTIC and CDRASTIC indices

**Table 7** Area of vulnerability ($km^2$ and %) identified by DRASTIC and CDRASTIC indices

| Vulnerability | DRASTIC | | | | CDRASTIC | | | |
|---|---|---|---|---|---|---|---|---|
| | Ranges | Area ($km^2$) | Area (%) | The aquifer geographic directions covered by the respective vulnerability | Ranges | Area ($km^2$) | Area (%) | The aquifer geographic directions covered by the respective vulnerability |
| Very low | 23-46 | 510.25 | 25.21 | Parts of the south, north, northwest, and northeast | <100 | 505.02 | 24.95 | Parts of the southeast, north, northwest, and northeast |
| Low | 47-92 | 775.14 | 38.31 | Parts of the south, southwest, southeast, north, northwest, northeast, and center | 100-145 | 817.70 | 40.41 | Parts of the south, southwest, southeast, north, northwest, northeast, and center |
| Moderate | 93-136 | 527. 85 | 26.08 | Parts of the south, southwest, northwest, and center | 145-190 | 524.06 | 25.89 | Parts of the south, southwest, southwest, northwest, and center |
| High | 137-184 | 171.02 | 8.46 | Parts of the northwest | 190-235 | 126.91 | 6.28 | Parts of the northwest and center |
| Very high | >185 | 39.23 | 1.94 | Parts of the northwest | ≥235 | 49.79 | 2.47 | Parts of the northwest |

### 3.3. Sensitivity of the DRASTIC Index

The MRSA, the DRASTIC index, is performed by eliminating the data of one layer at a time as indicated in Table 8. The results showed a high variation in the vulnerability index when the impact of the vadose zone was removed, such that the average variation index was 1.88%. This shows that the factor is more effective in vulnerability assessment using the DRASTIC index. When this parameter is removed from the overlay process, a significant decrease was observed in the vulnerability index. This could be due to the high theoretical weight assigned to this factor (weight = 5). These findings are similar to those obtained by Dibi et al. (2012) who have shown that, in addition to this parameter, topography, net recharge, and water table depth have a high impact on the vulnerability index. In addition, according to Samake et al. (2011), the vadose zone and hydraulic conductivity had a significant impact on the vulnerability index, that appears to have a moderate sensitivity to the deletion of water table depth (1.48%), net recharge (1.36%), and hydraulic conductivity (1.25%). The minimum menu variation index was achieved after eliminating the aquifer media (0.44%), as indicated in Table 8.

To estimate the effect of individual factors on aquifer vulnerability, the SPSA was performed. A summary of the results of SPSA in the DRASTIC index is given in Table 9. The SPSA

compares the effective and theoretical weights. The average effective weight of the net recharge was 43.26%, and its theoretical weight (%) was 17.4%. This shows that the factor is more effective in vulnerability assessment using the DRASTIC index. The results reported by other studies (Babiker et al., 2005; Doumouya et al., 2012) are similar to those of the present study. The water table depth and impact of the vadose zone parameters had high theoretical weights (21.74%), and have received an effective weight with the average value of 8.33% and 25.55% (Table 9). The remaining factors demonstrated an average effective weight of 14.91% (aquifer media), 9.89% (soil media), 11.35% (topography), and 7.01% (hydraulic conductivity). The theoretical weights assigned to the water table depth, net recharge, topography, and hydraulic conductivity were not in agreement with the effective weight. The highest and lowest impact on aquifer vulnerability belonged to net recharge and hydraulic conductivity, respectively (Table 9).

**Table 8** Statistical results of MRSA in the DRASTIC index

| The sensitivity of variability index (S) (%) | | | | Removed parameters |
|---|---|---|---|---|
| SD | Min. | Max. | Ave. | |
| 0.414 | 0.05 | 2.36 | 1.36 | D |
| 0.775 | 0.07 | 3.06 | 1.48 | R |
| 0.311 | 0.05 | 1.31 | 0.44 | A |
| 0.486 | 0.00 | 1.65 | 0.73 | S |
| 0.339 | 0.03 | 1.31 | 0.51 | T |
| 0.894 | 0.25 | 3.84 | 1.88 | I |
| 0.550 | 0.03 | 1.98 | 1.25 | C |

**Table 9** Statistical results of SPSA in the DRASTIC index

| Effective weight (%) | | | | Theoretical weight (%) | Theoretical Weight | Parameters |
|---|---|---|---|---|---|---|
| SD | Min. | Max. | Ave. | | | |
| 6.179 | 3.23 | 28.46 | 8.33 | 21.74 | 5 | D |
| 11.998 | 14.06 | 73.47 | 43.26 | 17.4 | 4 | R |
| 3.190 | 7.26 | 22.13 | 14.91 | 13.04 | 3 | A |
| 2.916 | 4.49 | 14.29 | 9. 89 | 8.7 | 2 | S |
| 2.222 | 6.45 | 14.71 | 11.35 | 4.3 | 1 | T |
| 5.367 | 15.79 | 37.31 | 25.55 | 21.74 | 5 | I |
| 3.738 | 2.42 | 18.75 | 7.01 | 13.04 | 3 | C |

### 3.4. Sensitivities of the CDRASTIC index

345 The MRSA in the CDRASTIC index was performed by eliminating one data layer at a time, as
346 indicated in Table 10. The mean variation index of hydraulic conductivity was 4.13%. Hydraulic
347 conductivity had the greatest effect on the aquifer vulnerability, followed by water table depth
348 (4.05%), soil media (3.82%), topography (3.68%), aquifer media (3.28%), net recharge (2.72%),
349 the impact of the vadose zone (2.33%), and land use (1.99%).

350 The effective weight derived from the SPSA to the CDRASTIC index is shown in Table 11.
351 The average effective weight of net recharge was 32.62%. This shows that the factor is more
352 effective in vulnerability assessment using CDRASTIC index. Hydraulic conductivity displays
353 the lowest effective weight (5.32%). Topography, net recharge, and land use parameters had the
354 maximum effective weights with respect to the theoretical weights specified for them. The
355 average effective weight of land use was 24.82%. This suggests that the parameter was the
356 second effective parameter in aquifer vulnerability, using the CDRASTIC index (Table 11).

357 **Table 10** Statistical results of MRSA in the CDRASTIC index

| The sensitivity of variability index (S) (%) | | | | Removed parameters |
|---|---|---|---|---|
| SD | Min. | Max. | Ave. | |
| 1.403 | 0.50 | 6.48 | 4.05 | D |
| 1.617 | 0.11 | 10.91 | 2.72 | R |
| 1.541 | 0.06 | 5.99 | 3.28 | A |
| 1.508 | 0.67 | 6.60 | 3.82 | S |
| 1.353 | 0.87 | 5.87 | 3.68 | T |
| 1.439 | 0.06 | 5.12 | 2.33 | I |
| 1.480 | 0.55 | 6.72 | 4.13 | C |
| 0.375 | 1.23 | 3.00 | 1.99 | L |

358 **Table 11** Statistical results of SPSA in the CDRASTIC index

| Effective weight (%) | | | | Theoretical weight (%) | Theoretical Weight | Parameters |
|---|---|---|---|---|---|---|
| SD | Min. | Max. | Ave. | | | |
| 4.849 | 2.63 | 26.88 | 6.27 | 21.74 | 5 | D |
| 10.672 | 10.4 | 66.67 | 32.62 | 17.4 | 4 | R |
| 3.026 | 6.29 | 20.00 | 11.23 | 13.04 | 3 | A |
| 2.621 | 3.31 | 12.96 | 7.5 | 8.7 | 2 | S |
| 1.609 | 5.2 | 12.82 | 8.45 | 4.3 | 1 | T |
| 4.648 | 10.87 | 32.05 | 19.2 | 21.74 | 5 | I |
| 3.134 | 2.1 | 14. 88 | 5.32 | 13.04 | 3 | C |
| 10.122 | 3.88 | 42.37 | 24.82 | 17.85 | 5 | L |

## 4. Conclusion

Evaluations of vulnerability indices for the Kerman–Baghin aquifer were conducted using the GIS-based DRASTIC and CDRASTIC indices. Seven hydro–geological factors (as the letters of the acronym show) were considered in the determination of aquifer vulnerability using DRASTIC, and eight parameters were considered in the CDRASTIC approach. From the DRASTIC index values, it was determined that 10.4% of the aquifer has high (8.46%) to very high (1.94%) vulnerability. From the CDRASTIC index values, it was determined that 8.75% of the aquifer has high (6.28%) to very high (2.47%) vulnerability. In addition, we found that parts of the north, south, southeast, and northwest have low to very low vulnerability based on the DRASTIC and CDRASTIC indices. The MRSA signifies that hydraulic conductivity and the impact of the vadose zone induce a high risk of aquifer contamination according to the DRASTIC and CDRASTIC indices, respectively. For both methods, the SPSA analysis revealed that net recharge has a high risk of aquifer contamination. Based on the results, parts of the Kerman–Baghin aquifer tend to be contaminated, a point which merits the attention of regional authorities. Regarding urban planning and the organization of agricultural activities in Kerman Province, the vulnerability map prepared in this study could be valuable in the protection of groundwater quality. In areas with high and very high vulnerability to groundwater pollution, there should be restrictions on soil fertilization as well as permanent pasture, or afforestation should be introduced in the arable land. In addition, these areas should not be converted into housing developments. Groundwater vulnerability maps of the Kerman–Baghin aquifer are ideal for use in future land-use planning.

*Data availability*. Data can be shared at this stage as authors are currently analysing for further work.

382 *Author contributions.* MN constructed an idea, planned methodology, interpreted results, and
383 then reached conclusions. MM supervised the whole process and provided personal,
384 environmental, and financial support for the research work. MN took responsibility for literature
385 review and finalising the whole paper and in the end critically reviewed the paper before
386 submission.

387 *Acknowledgments.* The authors would like to thank the Environmental Health Engineering
388 Research Center, Kerman University of Medical Sciences, for their scientific support.

389 *Competing interests.* The authors declare that they have no conflict of interest.

390 **References**

391 Aller, L., Truman, b., Jay H, L., Rebeeca J, P., and Glen, H.: DRASTIC: a standardized system
392 for evaluating ground water pollution potential using hydrogeologic settings, U.S Environmental
393 Protection Agency, USA, 1985.

394 Ayazi, M. H., Pirasteh, S., Arvin, A., Pradhan, B., Nikouravan, B., and Mansor, S.: Disasters and
395 risk reduction in groundwater: Zagros Mountain Southwest Iran using geoinformatics
396 techniques, Disaster Adv., 3, 51-57, 2010.

397 Baalousha, H.: Vulnerability assessment for the Gaza Strip, Palestine using DRASTIC, J.
398 Environ. Geol., 50, 405-414, https://doi.org/10.1007/s00254-006-0219-z, 2006.

399 Babiker, I. S., Mohamed, M. A., Hiyama, T., and Kato, K.: A GIS-based DRASTIC model for
400 assessing aquifer vulnerability in Kakamigahara Heights, Gifu Prefecture, central Japan, Sci
401 Total Environ., 345, 127-140, https://doi.org/10.1016/j.scitotenv.2004.11.005, 2005.

402 Baghapour, M. A., Talebbeydokhti, N., Tabatabee, H., and Nobandegani, A. F.: Assessment of
403 groundwater nitrate pollution and determination of groundwater protection zones using

DRASTIC and composite DRASTIC (CD) models: the case of Shiraz unconfined aquifer, J. Health. Sci. Surveill. Syst., 2, 54-65, 2014.

Baghapour, M. A., Nobandegani, A. F., Talebbeydokhti, N., Bagherzadeh, S., Nadiri, A. A., Gharekhani, M., and Chitsazan, N.: Optimization of DRASTIC method by artificial neural network, nitrate vulnerability index, and composite DRASTIC models to assess groundwater vulnerability for unconfined aquifer of Shiraz Plain, Iran, J Environ Health Sci Eng., 14, 1-16, https://doi.org/10.1186/s40201-016-0254-y, 2016.

Barber, C., Bates, L. E., Barron, R., and Allison, H.: Assessment of the relative vulnerability of groundwater to pollution: a review and background paper for the conference workshop on vulnerability assessment, AGSO J Aust Geol Geophys., 14, 147-154, 1993.

Boughriba, M., Barkaoui, A.-e., Zarhloule, Y., Lahmer, Z., El Houadi, B., and Verdoya, M.: Groundwater vulnerability and risk mapping of the Angad transboundary aquifer using DRASTIC index method in GIS environment, Arab J Geosci., 3, 207-220, https://doi.org/10.1007/s12517-009-0072-y, 2010.

Chitsazan, M., and Akhtari, Y.: Evaluating the potential of groundwater pollution in Kherran and Zoweircherry plains through GIS-based DRASTIC model, J. Water. Wastewater, 17, 39-51, 2006.

Chitsazan, M., and Akhtari, Y.: A GIS-based DRASTIC model for assessing aquifer vulnerability in Kherran Plain, Khuzestan, Iran, Water Resour Manag., 23, 1137-1155, https://doi.org/10.1007/s11269-008-9319-8, 2009.

Colins, J., Sashikkumar, M., Anas, P., and Kirubakaran, M.: GIS-based assessment of aquifer vulnerability using DRASTIC Model: A case study on Kodaganar basin, Earth Sci. Res. J., 20, 1-8, https://doi.org/10.15446/esrj.v20n1.52469, 2016.

427 Daly, D., and Drew, D.: Irish methodologies for karst aquifer protection, in: Beek B (ed)
428 Hydrogeology and engineering geology of sinkholes and karst, Balkema, Rotterdam, 267-272,
429 1999.
430 Dibi, B., Kouame, K. I., Konan-Waidhet, A. B., Savane, I., Biemi, J., Nedeff, V., and Lazar, G.:
431 Impact of agriculture on the quality of groundwater resources in peri-urban zone of Songon
432 (Cote D'ivoire), Environ. Engine. Manage. J., 11, 2173-2182,
433 https://doi.org/10.30638/eemj.2012.271, 2012.
434 Dixon, B.: Prediction of ground water vulnerability using an integrated GIS-based Neuro-Fuzzy
435 techniques, J. Spat. Hydro., 4, 1-38, 2004.
436 Doumouya, I., Dibi, B., Kouame, K. I., Saley, B., Jourda, J. P., Savane, I., and Biemi, J.:
437 Modelling of favourable zones for the establishment of water points by geographical information
438 system (GIS) and multicriteria analysis (MCA) in the Aboisso area (South-east of Côte d'Ivoire),
439 Environ. Earth. Sci., 67, 1763-1780, https://doi.org/10.1007/s12665-012-1622-2, 2012.
440 Ghazavi, R., and Ebrahimi, Z.: Assessing groundwater vulnerability to contamination in an arid
441 environment using DRASTIC and GOD models, Inte. J. Environ. Sci. Tech, 12, 2909-2918,
442 https://doi.org/10.1007/s13762-015-0813-2, 2015.
443 Ghosh, T., and Kanchan, R.: Aquifer vulnerability assessment in the Bengal alluvial tract, India,
444 using GIS based DRASTIC model, Model Earth Syst Environ., 2, 2-13,
445 https://doi.org/10.1007/s40808-016-0208-5, 2016.
446 Israil, M., Al-hadithi, M., Singhal, D., Kumar, B., Rao, M. S., and Verma, S.: Groundwater
447 resources evaluation in the Piedmont zone of Himalaya, India, using Isotope and GIS techniques,
448 J. Spatial. Hydro., 6, 107-119, 2006.

Jaiswal, R., Mukherjee, S., Krishnamurthy, J., and Saxena, R.: Role of remote sensing and GIS techniques for generation of groundwater prospect zones towards rural development--an approach, Int J Remote Sens., 24, 993-1008, https://doi.org/10.1080/01431160210144543, 2003.

Jaseela, C., Prabhakar, K., and Harikumar, P. S. P.: Application of GIS and DRASTIC modeling for evaluation of groundwater vulnerability near a solid waste disposal site, Int. J. Geoscien., 7, 558-571, https://doi.org/10.4236/ijg.2016.74043, 2016.

Javadi, S., Kavehkar, N., Mousavizadeh, M., and Mohammadi, K.: Modification of DRASTIC model to map groundwater vulnerability to pollution using nitrate measurements in agricultural areas, J. Agr. Sci. Tech., 13, 239-249, 2010.

Javadi, S., Kavehkar, N., Mohammadi, K., Khodadadi, A., and Kahawita, R.: Calibrating DRASTIC using field measurements, sensitivity analysis and statistical methods to assess groundwater vulnerability, Water. Int., 36, 719-732, https://doi.org/10.1080/02508060.2011.610921, 2011.

Jayasekera, D., Kaluarachchi, J. J., and Villholth, K. G.: Groundwater Quality Impacts Due to Population Growth and Land Use Exploitation in the Coastal Aquifers of Sri Lanka, Southern Illinois University Carbondale 2008, 43.

Jayasekera, D. L., Kaluarachchi, J. J., and Villholth, K. G.: Groundwater stress and vulnerability in rural coastal aquifers under competing demands: a case study from Sri Lanka, Environ Monit Assess. , 176, 13-30, https://doi.org/10.1007/s10661-010-1563-8, 2011.

Kardan Moghaddam, H., Jafari, F., and Javadi, S.: Vulnerability evaluation of a coastal aquifer via GALDIT model and comparison with DRASTIC index using quality parameters, Hydro. Sci. J., 62, 137-146, https://doi.org/10.1080/02626667.2015.1080827, 2017.

Kumar, P., Thakur, P. K., Bansod, B. K., and Debnath, S. K.: Assessment of the effectiveness of DRASTIC in predicting the vulnerability of groundwater to contamination: a case study from Fatehgarh Sahib district in Punjab, India, Environ. Earth. Sci., 75, 879, https://doi.org/10.1007/s12665-016-5712-4, 2016.

Madrucci, V., Taioli, F., and de Araújo, C. C.: Groundwater favorability map using GIS multicriteria data analysis on crystalline terrain, Sao Paulo State, Brazil, J. Hydro., 357, 153-173, https://doi.org/10.1016/j.jhydrol.2008.03.026, 2008.

Manap, M. A., Sulaiman, W. N. A., Ramli, M. F., Pradhan, B., and Surip, N.: A knowledge-driven GIS modeling technique for groundwater potential mapping at the Upper Langat Basin, Malaysia, Arabian. J. Geosci., 6, 1621-1637, https://doi.org/10.1007/s12517-011-0469-2, 2013.

Manap, M. A., Nampak, H., Pradhan, B., Lee, S., Sulaiman, W. N. A., and Ramli, M. F.: Application of probabilistic-based frequency ratio model in groundwater potential mapping using remote sensing data and GIS, Arabian. J.Geosci., 7, 711-724, https://doi.org/10.1007/s12517-012-0795-z, 2014a.

Manap, M. A., Nampak, H., Pradhan, B., Lee, S., Sulaiman, W. N. A., and Ramli, M. F.: Application of probabilistic-based frequency ratio model in groundwater potential mapping using remote sensing data and GIS, Arabian. J. Geosci., 7, 711-724, https://doi.org/10.1007/s12517-012-0795-z, 2014b.

Martínez-Bastida, J. J., Arauzo, M., and Valladolid, M.: Intrinsic and specific vulnerability of groundwater in central Spain: the risk of nitrate pollution, Hydro. J., 18, 681-698, https://doi.org/10.1007/s10040-009-0549-5, 2010.

Merchant, J. W.: GIS-based groundwater pollution hazard assessment: a critical review of the DRASTIC model, Photogramm Eng Remote Sensing., 60, 1117-1127, 1994.

494 Modabberi, H., Hashemi, M. M. R., Ashournia, M., and Rahimipour, M. A.: Sensitivity Analysis
495 and Vulnerability Mapping of the Guilan Aquifer Using Drastic Method, Rev. Environ. Earth.
496 Sci., 4, 27-41, https://doi.org/10.18488/journal.80.2017.41.27.41, 2017.
497 Napolitano, P., and Fabbri, A.: Single-parameter sensitivity analysis for aquifer vulnerability
498 assessment using DRASTIC and SINTACS, Proceedings of the Vienna Conference,
499 Netherlands, 1996, 559-566.
500 National Research Council: Ground water vulnerability assessment: Predicting relative
501 contamination potential under conditions of uncertainty. National Academies Press, USA, 224,
502 1993.
503 Neshat, A., Pradhan, B., Pirasteh, S., and Shafri, H. Z. M.: Estimating groundwater vulnerability
504 to pollution using a modified DRASTIC model in the Kerman agricultural area, Iran, Environ.
505 Earth. Sci., 71, 3119-3131, https://doi.org/10.1007/s12665-013-2690-7, 2014.
506 Neshat, A., and Pradhan, B.: Evaluation of groundwater vulnerability to pollution using
507 DRASTIC framework and GIS, Arabian. J. Geosci., 10, 2-8, https://doi.org/10.1007/s12517-017-
508 3292-6, 2017.
509 Raju, N. J., Ram, P., and Gossel, W.: Evaluation of groundwater vulnerability in the lower
510 Varuna catchment area, Uttar Pradesh, India using AVI concept, J. Geol. Soc. India., 83, 273-
511 278, https://doi.org/10.1007/s12594-014-0039-9, 2014.
512 Saida, S., Tarik, H., Abdellah, A., Farid, H., and Hakim, B.: Assessment of groundwater
513 vulnerability to nitrate based on the optimised DRASTIC models in the GIS Environment (Case
514 of Sidi Rached Basin, Algeria), Geosciences, 7, 2-23,
515 https://doi.org/10.3390/geosciences7020020, 2017.

Saidi, S., Bouri, S., and Ben Dhia, H.: Sensitivity analysis in groundwater vulnerability assessment based on GIS in the Mahdia-Ksour Essaf aquifer, Tunisia: a validation study, Hydro. Sci. J., 56, 288-304, https://doi.org/10.1080/02626667.2011.552886, 2011.

Samake, M., Tang, Z., Hlaing, W., Mbue, I. N., Kasereka, K., and Balogun, W. O.: Groundwater vulnerability assessment in shallow aquifer in Linfen Basin, Shanxi Province, China using DRASTIC model, J. Sustain. Develop., 4, 53-71, https://doi.org/10.5539/jsd.v4n1p53, 2011.

Sarah, C., and Patricia l, C.: Ground water vulnerability assessment: Predicting relative contamination potential under conditions of uncertainty, National Academies Press, USA, 1993.

Secunda, S., Collin, M., and Melloul, A. J.: Groundwater vulnerability assessment using a composite model combining DRASTIC with extensive agricultural land use in Israel's Sharon region, J. Environ. Manage., 54, 39-57, https://doi.org/10.1006/jema.1998.0221, 1998.

Shirazi, S. M., Imran, H., and Akib, S.: GIS-based DRASTIC method for groundwater vulnerability assessment: a review, J. Risk. Res., 15, 991-1011, https://doi.org/10.1080/13669877.2012.686053, 2012.

Singh, A., Srivastav, S., Kumar, S., and Chakrapani, G. J.: A modified-DRASTIC model (DRASTICA) for assessment of groundwater vulnerability to pollution in an urbanized environment in Lucknow, India, Environ. Earth. Sci., 74, 5475-5490, https://doi.org/10.1007/s12665-015-4558-5, 2015.

Souleymane, K., and Tang, Z.: A novel method of sensitivity analysis testing by applying the DRASTIC and fuzzy optimization methods to assess groundwater vulnerability to pollution: the case of the Senegal River basin in Mali, Nat. Hazards. Earth. Sys. Sci., 17, 1375-1392, https://doi.org/10.5194/nhess-17-1375-2017, 2017.

538 Srivastava, P. K., and Bhattacharya, A. K.: Groundwater assessment through an integrated
539 approach using remote sensing, GIS and resistivity techniques: a case study from a hard rock
540 terrain, Int. J. Remote. Sens., 27, 4599-4620, https://doi.org/10.1080/01431160600554983,
541 2006.
542 Tilahun, K., and Merkel, B. J.: Assessment of groundwater vulnerability to pollution in Dire
543 Dawa, Ethiopia using DRASTIC, Environ. Earth. Sci., 59, 1485-1496,
544 https://doi.org/10.1007/s12665-009-0134-1, 2010.
545 Zghibi, A., Merzougui, A., Chenini, I., Ergaieg, K., Zouhri, L., and Tarhouni, J.: Groundwater
546 vulnerability analysis of Tunisian coastal aquifer: an application of DRASTIC index method in
547 GIS environment, Groundwater. Sustain. Develop., 2, 169-181,
548 https://doi.org/10.1016/j.gsd.2016.10.001, 2016.

549